

**„VICTOR BABEȘ” UNIVERSITY OF MEDICINE AND
PHARMACY TIMIȘOARA
FACULTY OF PHARMACY
DEPARTAMENT II**

GHIULAI ROXANA MARIA



ABSTRACT

**HIGH-PERFORMANCE ANALYTICAL AND
BIOLOGICAL STUDIES REGARDING THE
PHARMACOLOGICAL PROPERTIES OF
BETULINIC ACID**

Scientific coordinator

PROF. UNIV. DR. ȘOICA CODRUȚA

**Timișoara
2022**

TABLE OF CONTENTS

LIST OF PUBLISHED SCIENTIFIC PAPERS	VI
LIST ABBREVIATIONS AND SYMBOLS	VIII
LIST OF FIGURES	X
LIST OF TABLES	XII
ACKNOWLEDGEMENTS	XIII
INTRODUCTION	XIV
GENERAL PART	1
1. PENTACYCLIC TRITERPENES	1
2. BETULINIC ACID	4
2.1. CHEMICAL STRUCTURE	4
2.2. EXTRACTION METHODS	6
2.3. CHEMICAL SYNTHESIS	7
2.4. BIOLOGICAL ACTIVITIES OF BETULINIC ACID	8
2.4.1. ANTICANCER ACTIVITY	9
2.4.2. ANTIINFLAMMATORY ACTIVITY	13
2.4.3. WOUND HEALING	16
2.4.4. ANTIDIABETIC ACTIVITY	17
2.4.5. CARDIOPROTECTIVE ACTIVITY	17
2.4.6. LIPOLYTIC ACTIVITY	18
2.4.7. VARIOUS BIOLOGICAL ACTIVITIES	19
2.5. NANO-SCALE DELIVERY SYSTEMS FOR BETULINIC ACID	20
2.5.1. NANOEMULSIONS	21
2.5.2. METALLIC NANOPARTICLES	21
2.5.3. LIPOSOMES	22
2.5.4. POLYMERIC NANOPARTICLES	23
2.5.5. CARBON NANOTUBES	24
2.5.6. CYCLODEXTRIN COMPLEXES	24
3. ANALYTICAL INVESTIGATIONS OF PHARMACOKINETIC PARAMETERS	25
3.1. STATE OF ART IN METABOLOMICS	25
SPECIAL PART	27
4. <i>IN VIVO</i> METABOLIC PATHWAY OF BETULINIC ACID	27
4.1. OBJECTIVES	27
4.2. MATERIALS AND METHODS	28
4.2.1. CHEMICALS	28
4.2.2. BA NANOEMULSION	28
4.2.3. <i>IN VIVO</i> EXPERIMENT ON SKH1 MICE	29
4.2.4. SAMPLE PREPARATION FOR LC-MS ANALYSIS	29

4.2.5. SAMPLE PREPARATION FOR HRMS ANALYSIS.....	30
4.2.6. HPLC-MS APPARATUS	30
4.2.7. LC-MS METHODS.....	30
4.2.8. ORBITRAP MASS SPECTROMETRY.....	31
4.3. RESULTS	32
4.3.1. IDENTIFICATION AND QUANTIFICATION OF BETULINIC ACID FROM PLASMA SAMPLES.....	32
4.3.2. HRMS SCREENING OF BETULINIC ACID PHASE I PLASMA METABOLITES OF BY NANOESI ORBITRAP MS	35
4.3.3. HRMS SCREENING OF BETULINIC ACID PHASE II PLASMA METABOLITES OF BY NANOESI ORBITRAP MS	37
4.3.4. TANDEM MS ANALYSIS OF BETULINIC ACID AND ITS PLASMA METABOLITES BY CID NANOESI ORBITRAP MS	38
4.3.4.1. Tandem MS analysis of betulinic acid isolated from plasma samples	38
4.3.4.2. Tandem MS analysis of betulinic acid phase I metabolites isolated from plasma samples	41
4.3.4.3. Tandem MS analysis of betulinic acid phase II metabolites isolated from plasma samples	49
4.3.4.3.1. Tandem MS analysis of methylated metabolites	49
4.3.4.3.2. Tandem MS analysis of sulphated metabolites	51
4.3.4.3.3. Tandem MS analysis of glucuronoconjugated metabolites	59
4.4. DISCUSSION.....	67
5. DESIGN, SYNTHESIS AND PHYSICO-CHEMICAL CHARACTERISATION OF BETULINIC ACID GOLD NANOPARTICLES.....	74
5.1. OBJECTIVES.....	74
5.2. MATERIALS AND METHODS.....	75
5.2.1. SYNTHESIS OF CITRATE-CAPPED GOLD NANOPARTICLES (GNP)	75
5.2.2. SYNTHESIS OF BA-LOADED GOLD NANOPARTICLES (BA-GNP).....	75
5.2.3. CHARACTERIZATION OF GNP AND BA-GNP BY UV-VIS, FTIR, TEM, HYDRODYNAMIC SIZE, ZETA POTENTIAL	76
5.2.4. GNP'S GOLD CONTENT ASSESSMENT BY X-RAY FLUORESCENCE (XRF) ANALYSIS	77
5.2.5. DRUG LOADING EFFICIENCY ASSESSMENT	77
5.3. RESULTS	78
5.3.1. SYNTHESIS OF CITRATE-CAPPED GNP AND BA-GNP.....	78
5.3.2. UV-VIS CHARACTERIZATION OF GNP AND BA-GNP.....	79
5.3.3. FTIR CHARACTERIZATION OF GNP AND BA-GNP	80
5.3.4. TRANSMISSION ELECTRON MICROSCOPY (TEM), DYNAMIC LIGHT SCATTERING (DLS), ZETA POTENTIAL (Z), DRUG LOADING EFFICIENCY (DLE) AND GOLD CONTENT OF GNP	81
5.4. DISCUSSION.....	83

6. <i>IN VITRO</i> AND <i>IN OVIO</i>BIOLOGICAL ASSESSMENT OF BETULINIC ACID GOLD NANOPARTICLES.....	86
6.1. OBJECTIVES.....	86
6.2. MATERIALS AND METHODS.....	86
6.2.1. CELL CULTURE.....	86
6.2.2. 3D TISSUE MODELS (EPI-200 AND EPI-200-SIT, MATTEK LIFE SCIENCES)	87
6.2.3. CELL VIABILITY ASSESSMENT BY ALAMAR BLUE ASSAY AND CELL MORPHOLOGY	87
6.2.3.1. Alamar Blue Staining.....	87
6.2.3.2. Cellular morphology evaluation	88
6.2.4. RECONSTRUCTED HUMAN EPIDERMAL MODEL (EPI-SIT-MD)—SKIN IRRITATION OF MEDICAL DEVICE EXTRACTS ASSAY	88
6.2.5. EPIDERMAL SKIN MODEL (EPI 200)—PHOTOTOXICITY TEST.....	89
6.2.6. IMMUNOFLUORESCENCE ASSAY	90
6.2.7. HET-CAM ASSAY	90
6.2.8. HIGH-RESOLUTION RESPIROMETRY	91
6.2.9. WESTERN BLOT	93
6.3. RESULTS	94
6.3.1. EFFECT OF GNP AND BA-GNP ON CELL VIABILITY AND MORPHOLOGY.....	94
6.3.2. MORPHOLOGICAL ASSESSMENT OF APOPTOTIC CELLS BY DAPI STAINING.....	97
6.3.3. GNP AND BA-GNP EFFECTS ON HACAT AND RPMI-7951 MITOCHONDRIAL RESPIRATION.....	98
6.3.4. WESTERN BLOT	100
6.3.5. EFFECT OF GNP AND BA-GNP ON RECONSTRUCTED HUMAN EPIDERMAL MODEL (EPI-SIT-MD)—SKIN IRRITATION OF MEDICAL DEVICE EXTRACTS ASSAY	102
6.3.6. EFFECT OF GNP AND BA-GNP ON EPIDERMAL SKIN MODEL (EPI 200)—PHOTOTOXICITY TEST.....	103
6.3.7. IRRITATION POTENTIAL OF BA-GNP USING THE HET-CAM ASSAY	104
6.4. DISCUSSION.....	105
CONCLUSIONS AND PERSONAL CONTRIBUTIONS	110
REFERENCES	113
<i>IN EXTENSO</i> PUBLISHED ARTICLES.....	I

ABSTRACT

Betulinic acid (BA) (3 β , hydroxy-lup-20(29)-en-28-oic acid) (Figure 1) is a secondary plant metabolite, member of lupane-skeleton pentacyclic triterpenes. BA is widely distributed in natural occurring sources, considerable amounts being found throughout Betulaceae species, in the outer layers of birch bark. Some vegetal sources with high amounts of BA are an important part of natural remedies that include traditional chinese medicine such as *Ziziphi Spinosae semen* (Rhamnaceae) or indian medicinal remedies such as *Nyctanthes arbor-tristis*.

In the last decades BA was extensively investigated during *in vitro* and *in vivo* studies that demonstrated a wide range of biological and pharmacological activities, the most high profile being its anti-cancer potential, already recognized by the National Cancer Institute of USA. BA displays well documented cytotoxicity activities mainly by triggering the mitochondrial pathway of apoptosis in cancer cells exerted on various types of cancers such as melanoma, colorectal cancer, ovarian cancer, cervical cancer or breast cancer. Hence BA has an immense potential of becoming an antineoplastic agent that combines high anti-cancer activity, low overall toxicity and high selectivity.

One major drawback of BA is represented by its low water solubility which negatively affects its oral bioavailability thus limiting its pharmacological activity. To overcome these shortcomings and to improve its pharmacokinetic features, a lot of strategies have been employed to develop nano-scale delivery systems among which cyclodextrin complexation and several nanoformulations containing BA, among which liposomes, nanoemulsions, metallic nanoparticles, carbon nanotubes (Figure 2).

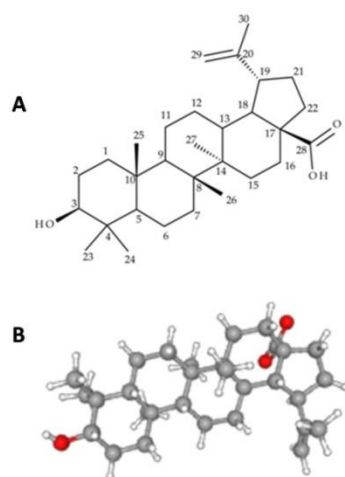


Figure 1.Chemical structure of betulinic acid. (A) 2D structure. (B) 3D structure

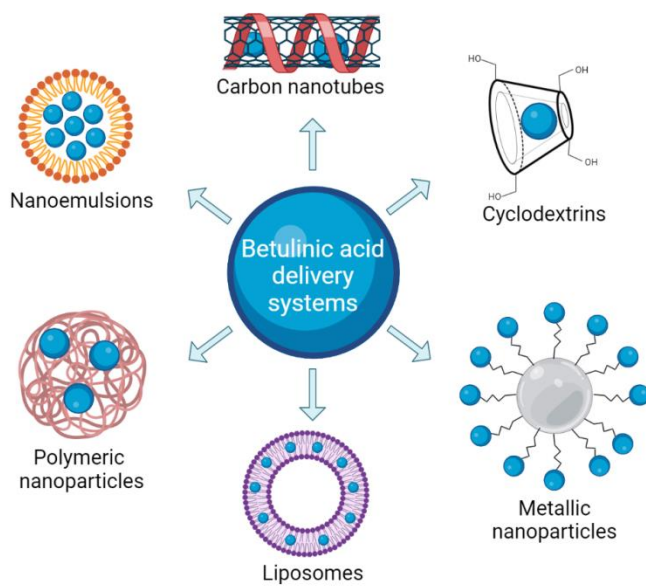


Figure 2. Betulinic acid nano-scale delivery systems

In drug development, a mandatory stage lies in disclosing its complete pharmacokinetic parameters, such as absorption, distribution, metabolism and excretion, briefly its ADME profile. Despite the remarkable results in disclosing the underlying molecular mechanisms for most of BA biological and pharmacological activities during *in vitro* and *in vivo* studies, there is limited information regarding its *in vivo* ADME profile.

The main objectives during the present doctoral thesis, which represent the special part of the doctoral thesis was to address BAs shortcomings and to complete the gap of information regarding its pharmacological characteristics. To this purpose, **three studies** were conducted having betulinic acid as their central point. To complete the pharmacokinetic profile of BA with insights on their metabolic transformation *in vivo*, an ample **first study** was conducted that consisted in the screening and structural investigations of its phase I and phase II metabolites. To address BAs poor bioavailability, a **second study** was conducted which consisted in the synthesis of BA loaded gold nano-particles (BA-GNP), which were thoroughly characterized and investigated in terms of identity, stability and drug loading efficiency, that have the credentials to boost the bioavailability also enhance its therapeutic efficacy. Biological *in vitro* assessment of the newly obtained BA and its functionalized GNP was the focus of the **third study**, which was conducted on human melanoma cells that revealed selective cytotoxic properties and stronger antiproliferative effects compared to free BA, while lacking irritation potential on normal cells/tissues. Moreover, the underlying antimelanoma mechanism was revealed by means of high throughput biological tests.

During the first study a previously developed BA-containing nanoemulsion (BA-NE) was IP administered within the peritoneal cavity to SKH1 female mice. Following *in vivo* administration, the research was focused on: i) its detection and quantification in plasma samples by LC-MS ii) the screening and sequencing of BA metabolites using HRMS, by nanoESI Orbitrap MS in negative ion mode, and

structural characterisation was achieved by CID MS/MS. Results indicated that the LC-MS method provided high sensitivity in detecting BA even after low dosage in mice. Plasma samples with the highest BA detected concentrations, collected after 2h post treatment, were further analyzed by HRMS to unravel the in vivo metabolic pathway of BA. The study design, in conjunction with the analytical method used, enabled the detection of 13 BA phase I and phase II metabolites in plasma samples. Oxidation, monohydroxylation, dihydroxylation, and hydrogenation were the primary metabolic pathways during BA's phase I metabolism while sulfation, glucuronidation, and methylation were the primary metabolic processes during phase II (Table 1).

Table 1. Proposed phase I and phase II metabolic products of betulinic acid

Metabolite	Molecular formula	<i>m/z</i>	Molecular ion	Metabolic reaction
M 1	C ₃₀ H ₅₀ O ₃	457.37	[M-H ⁺] ⁻	- hydrogenation
M 2	C ₃₀ H ₄₈ O ₄	471.35	[M-H ⁺] ⁻	- monohydroxylation
M 3	C ₃₀ H ₄₆ O ₅	485.33	[M-H ⁺] ⁻	- oxydation
M 4	C ₃₀ H ₄₈ O ₅	487.34	[M-H ⁺] ⁻	- dihydroxylation
M 5	C ₃₁ H ₅₀ O ₃	469.37	[M-H ⁺] ⁻	- methylation
M 6	C ₃₀ H ₄₈ O ₆ S	535.31	[M-H ⁺] ⁻	- sulfoconjugation
M 7	C ₃₀ H ₄₈ O ₇ S	551.30	[M-H ⁺] ⁻	- hydroxylation - sulfoconjugation
M 8	C ₃₀ H ₄₆ O ₈ S	565.28	[M-H ⁺] ⁻	- oxidation - sulfoconjugation
M 9	C ₃₀ H ₄₈ O ₈ S	567.30	[M-H ⁺] ⁻	- dihydroxylation - sulfoconjugation
M 10	C ₃₆ H ₅₆ O ₉	631.39	[M-H ⁺] ⁻	- glucuronidation
M 11	C ₃₆ H ₅₆ O ₁₀	647.38	[M-H ⁺] ⁻	- hydroxylation - glucuronidation
M 12	C ₃₆ H ₅₄ O ₁₁	661.36	[M-H ⁺] ⁻	- oxydation - glucuronidation
M 13	C ₃₆ H ₅₆ O ₁₁	663.37	[M-H ⁺] ⁻	- dihydroxylation - glucuronidation

During the detailed structural analysis by nanoESI CID MS/MS, the main fragmentation features disclosed for both BA and its metabolites consisted in neutral losses of H₂O (- 18 Da), CO₂ (- 44 Da), HCOOH (- 46 Da), C₃H₄ (-40 Da), O (-16 Da), CH₂(-14Da) and ring cleavage fragment ions, as already reported for phytocompounds such as triterpenes and triterpenic acids. Obtained results indicate the formation of a large number of diagnostic fragment ions that are consistent with the proposed structures of analyzed metabolites. A comparative assessment of the fragmentation schemes discloses that all the metabolites follow a fragmentation pattern similar to the one of BA (Figure 3).

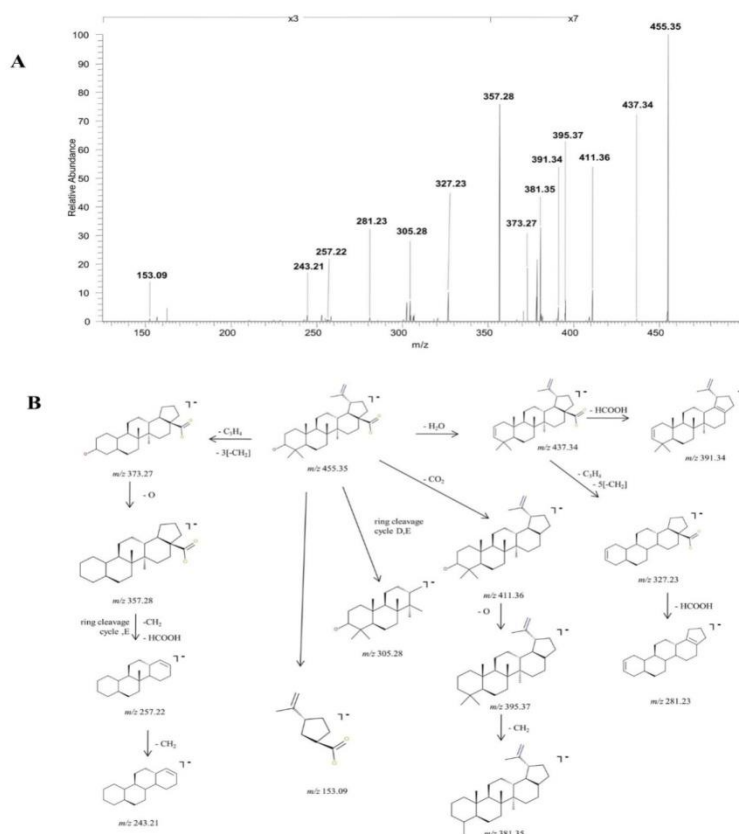


Figure 3. Structural characterization of betulinic acid (BA) (A) ESI CID MS/MS spectra of the [M-H]⁻ ion detected at m/z 455.35 in the negative ion mode (B) Proposed fragmentation pathway.

All combined, the obtained results deliver new information regarding the *in vivo* metabolic pathway of BA and document the fragmentation pathway of BA and its metabolites. The current study contributes to elucidate the metabolomic profile of BA and can represent a support for future studies.

To address BAs poor bioavailability, a second study was conducted which consisted in the synthesis of BA loaded gold nano-particles (BA-GNP) that have the credentials to boost the bioavailability also enhance its therapeutic efficacy. Using cysteamine as a link, BA was grafted onto previously synthesized citrate-capped GNP to produce BA-GNP (Figure 4). BA-GNP were thoroughly characterized and investigated in terms of identity (by UV-VIS, FTIR, TEM, DLS, Z potential), stability and drug loading efficiency

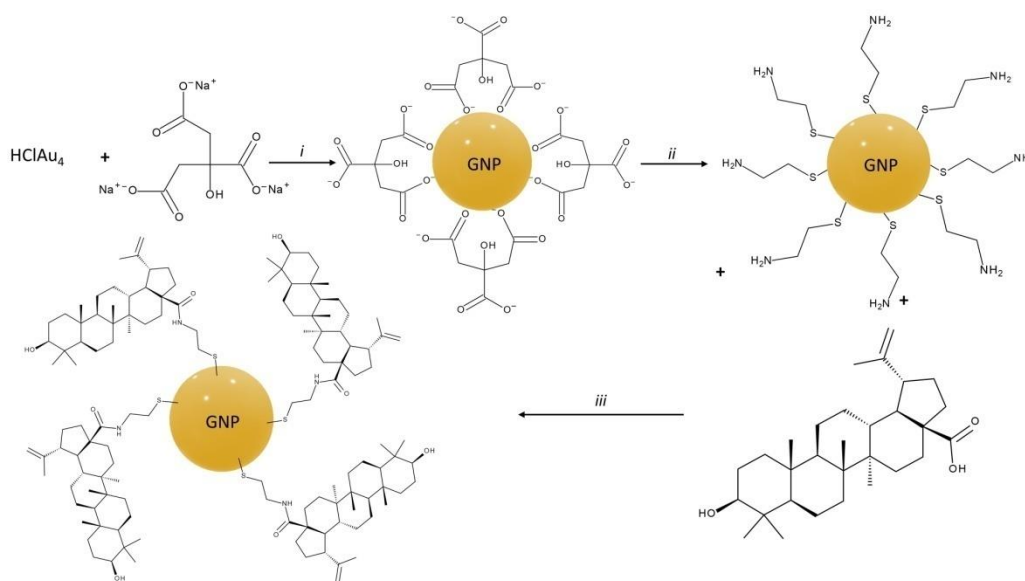


Figure 4. Synthesis route for citrate-capped GNP and BA-GNP

Biological *in vitro* assessment of the newly obtained BA and its functionalized GNP was the focus of the third study, which was conducted on HaCaT human keratinocytes and RPMI-7951 human melanoma cells. The biological tests conducted on BA-GNP assessed their effect on cell viability and morphology, irritation potential or their effect on mitochondrial respiration. Cell viability results indicated selective cytotoxic properties, experimental data revealing the lack of cytotoxic effects on HaCaT human keratinocytes and stronger antiproliferative effects on RPMI-7951 human melanoma cells compared to free BA against melanoma cells (Figure 5). The Alamar Blue oxidation-reduction indicator, which quantifies cell viability by changing color in response to chemical reduction due to cell growth, revealed a significant dose-dependent cell death percentage after the application of BA-GNP samples. Of note, cell viability decreased more pronouncedly when conjugated BA was tested compared to the BA alone, thus indicating that the presence of the phytochemical indeed plays a key role in the inhibitory process and that its penetration into the cancer cells is facilitated by the metallic nanocarrier.

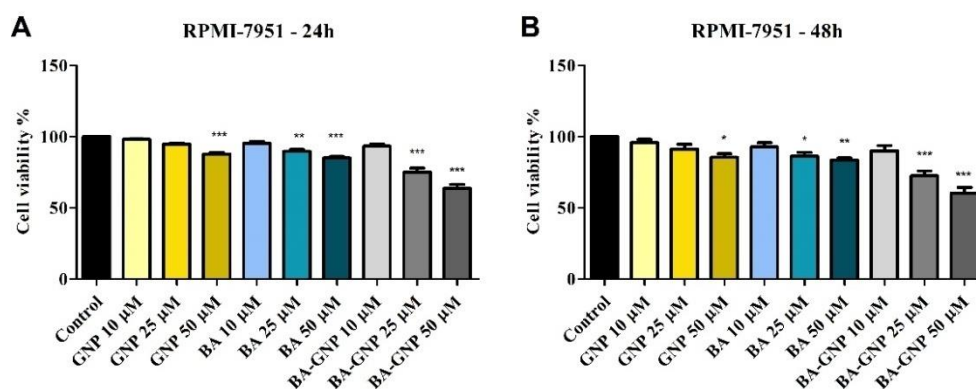


Figure 5. Cell viability of RPMI-7951 cells after 24h (A) and 48h (B) treatment with GNP (diluted to match the same gold content as for BA loaded NPs at 10, 25 and 50 µM), BA and BA-GNP (10, 25 and 50 µM). The results are expressed as cell viability percentage (%) normalized to control (100%). The data represent the mean values \pm SD of three independent experiments performed in triplicate. The statistical differences vs. control was determined using one-way ANOVA analysis followed by Tukey's multiple comparisons post-test (* $p < 0.05$, ** $p < 0.005$ and *** $p < 0.0001$).

Further, pro-apoptotic effects were disclosed by DAPI staining. Apoptotic changes such as nuclear condensation, shrinkage and fragmentation in a dose-dependent manner were revealed only for the phytochemical-conjugated GNP, while the naked GNP left the nuclei unaltered that were corroborated by western blot data demonstrating the down-regulation of anti-apoptotic Bcl-2 expression and the up-regulation of pro-apoptotic Bax. BA-GNP also decreased mitochondrial respiration considerably, demonstrating their mitochondria-specific action (Figure 6).

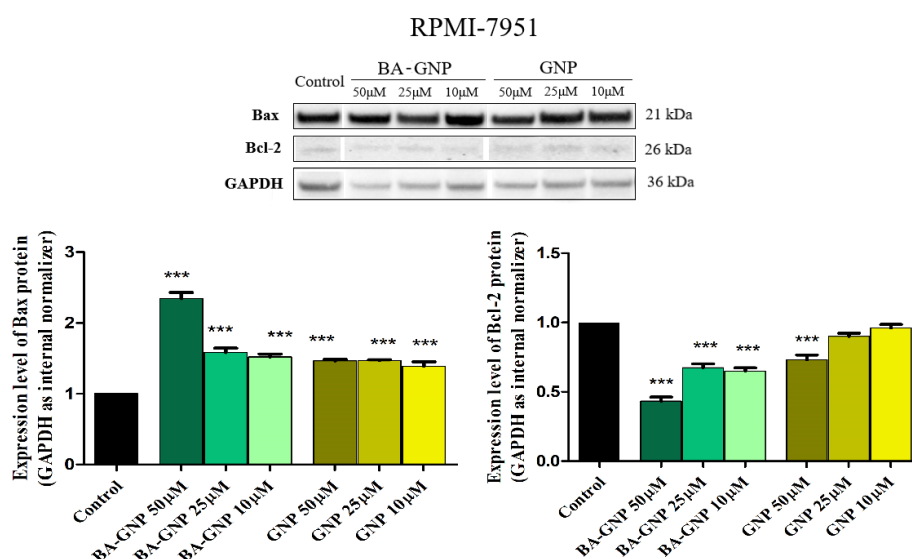


Figure 6. Determination of Bax and Bcl-2 protein expression in RPMI-7951 cells. Protein extracts from whole cells were prepared and equal amounts of protein (25 μg per lane) were separated by Bolt™ 4–12%, Bis-Tris, and polyacrylamide gels. After transfer on the nitrocellulose membrane, immunodetection was carried out using anti-Bcl-2 and anti-Bax antibodies. The data represent the mean values ± SD of three independent experiments after normalization against the GAPDH loading control and the control group. The statistical differences vs. control were determined using one-way ANOVA analysis followed by Tukey's multiple comparisons post-test (***) $p < 0.0001$.

High-resolution respirometry studies were conducted in both melanoma cells and human keratinocytes in order to assess the underlying mechanism of action for the BA-GNP. Experimental data showed that neither BA-GNP nor naked GNP had any significant influence on mitochondrial respiration in HaCaT cells when used in low concentrations. In RPMI-7951 melanoma cells, data showed that BA-GNP produced a significant reduction of all respiratory rates together with an increase of Cyt c rate. Moreover, BA-GNP inhibits active respiration ($\text{OXPHOS}_{\text{CI}}$ and $\text{OXPHOS}_{\text{CI+CI}}$) and also the maximal respiratory capacity of the electron transport chain (ETS_{CI} and $\text{ETS}_{\text{CI+CI}}$), thus demonstrating impairment of mitochondrial function. Similar effects were elicited by naked GNP in RPMI-7951 cells, but only when the highest concentration was used.

Irritation potential of BA-GNP was conducted using the HET-CAM assay (Figure 7) and EPI-SIT-MD skin irritation assay while the phototoxic potential was assessed during EPI 200 phototoxicity test. Results indicated that GNP can be considered biocompatible with mucosal tissues and a safe type of BA nanoformulation for local applications, while non-irritant and no-phototoxic potential on 3D reconstructed human epidermal models.

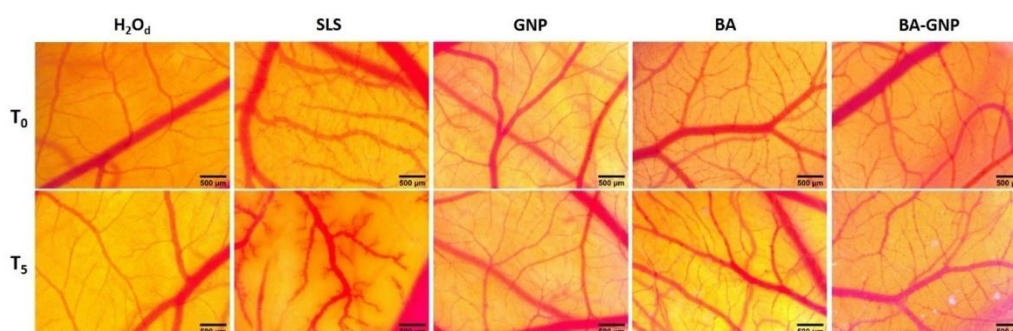


Figure 7. Irritation potential assessment using the HET-CAM method after treatment with GNP, BA and BA-GNP. Stereomicroscope images show the in-face chorioallantoic membrane before (T_0) and 300 s after application (T_5) of 300 μL of the test sample in concentrations of 1 μM and control samples (distilled water H_2O as negative control, SLS 0.5% as positive control and DMSO 0.5% as solvent control); scale bars represent 500 μm .

All of the obtained results combined contribute to enrich BA's existing pharmacological profile with both pharmacokinetic data and with underlying molecular mechanisms of their anticancer activity. Moreover, these studies represent a ground work for future perspectives in obtaining efficient derivatives or innovative nano-scale delivery systems for BA with improved bioavailability and enhanced pharmacological activity